Open Access Library Journal
2024, Volume 11, e11461
ISSN Online: 2333-9721
ISSN Print: 2333-9705

Synthetic Analysis of the Methanol-Raphia-Sese Oil Interface with a View to Obtaining Biodiesel under Chemcad Software

—Case of Acid or Base Transesterification

Biabongo N. Pamphile[1], Emmanuel Neva Okwes[2], Gedeon Ekulu[3]

[1]Department of Process Engineering in Refining and Petrochemistry, Faculty of Gas, Oil and Renewable Energy, University of Kinshasa, Kinshasa, DRC
[2]Process Engineering and Thermodynamics Laboratory (LGPT), Kinshasa, DRC
[3]University of Lorraine, Nancy, Metz, Epinal, Thionville, Grand Est, France
Email: pamphilebiabongo@gmail.com, Gekulu@yahoo.fr

How to cite this paper: Pamphile, B.N., Okwes, E.N. and Ekulu, G. (2024) Synthetic Analysis of the Methanol-Raphia-Sese Oil Interface with a View to Obtaining Biodiesel under Chemcad Software. *Open Access Library Journal*, **11**: e11461.
https://doi.org/10.4236/oalib.1111461

Received: March 20, 2024
Accepted: October 27, 2024
Published: October 30, 2024

Abstract

In this paper, the biodiesel starting from raphia-sese oil in the presence of a methanol was obtained. On this, a model of the explanatory circuit was established on basis of which the assessment matter takes shape according to the quantity and intrinsic properties of products. The results obtained with this model were validated and, one thus could confirm the properties of the product under interfaces: temperature-density, temperature-viscosity, temperature-pressure, mass temperature-heat and temperature-conductivity. This circuit is a result, which constitutes a base of the data that will be able to extend to other oils and alcohol according to whether one wants to obtain by acid or basic cross esterification. To bring the precision to the result of reaction, we were used for ourselves the literature of preliminary raphia established in [1].

Subject Areas

Analytical Chemistry

Keywords

Acid Cross Esterification, Oil Raphia-Sese, Software Chemcad

1. Introduction

The energy accessibility is the first challenge of this century. More forms of resources are used to produce energy. However, the environment pollution due to

the usage of fossil fuels is the main problem that must be solved for these decades. Many scientists propose a diversification of the energy production by using raw vegetable materials that are renewable and sustainable [2] [3].

The former researches focused on quality analysis, such as this one about the physicochemical properties of the extracted oil from Raffia palm (*Raphia regalis*), were investigated. Physical properties such as refractive index, specific gravity, viscosity, moisture content, flash point, smoke point, fire point, pour point and cloud point; and chemical properties such as acid value, free fatty acid, saponification value, unsaponifiable matter, iodine value, ester value and peroxide value were investigated for both raw Raffia oil and transesterified raffia oil. The various properties were investigated using ASTM standard methods and calculations. Results obtained for physical properties: refractive index, specific gravity, viscosity, moisture content, flash point, smoke point, fire point, pour point and cloud point were 1.437, 0.765, 1.420 mm^2/sec, 8.0%, 154Â˚C, 140Â˚C, 160Â˚C, −3Â˚C and -7Â˚C respectively for the raw Raffia oil, and 1.341, 0.840, 1.21 mm^2/sec, 1.6%, 70Â˚C, 66Â˚C, 72Â˚C, −5Â˚C and −12Â˚ for the transesterified raffia oil. Results for the chemical properties: acid value, free fatty acid, saponification value, ester value obtained in (mgKOH/g), iodine value (mgI^2/g), peroxide value (mEq/kg) and unsaponifiable matter (%) were determined to be 18.849, 9.472, 136.043, 117.194, 5.076, 192.000 and 1.814% respectively for the raw Raffia oil; and 31.977, 16.069, 193.545, 161.568, 167.50, 350.800 and 2.481% for the transesterified raffia oil. It was concluded that Raffia oil when processed has great potential for use as alternative fuel for energy generation [1].

The establishment of a precise circuit for obtaining biodiesel based on raffia sese oils is of paramount importance since it allows us to better identify the different stages of transformation and would promote the nutritive use of oils from palm instead of their use in biodiesel. On this, we highlight the following aspects: first, the contradictory results of different reviews of the literature on the energy and environmental balance of biodiesel, then the quantitative production of these oils. To do this, the physico-chemical properties are taken in [1] [4].

2. Methodology

The experimental aspect is based on software and interpreted by the mathematical language of fluid mechanics. The different solutions are obtained by digital simulation and modeling by implementing the different values obtained, the results follow exponential and linear trend curves. However, the type of transesterification was chosen, because the biodiesel obtained separates easily from glycerol and oil. This means that the biodiesel and glycerol obtained are pure and can be sold without further processing.

3. Results and Discussion

3.1. Acid or Base Transesterification

It is a chemical reaction during which an ester is transformed into another ester.

This reaction can be catalyzed by a base or an acid. Each molecule of triglycerides produces three molecules of ester called mono-esters according to Equation (1) below [5]:

$$\begin{array}{cccccccc} H_2 & -C- & OCOR' & & & ROCOR' & & H_2C-OH \\ & | & & & & & & | \\ H & -C- & OCOR'' & +3ROH & \xrightarrow{KOH} & ROCOR'' & + & H'C-OH \\ & | & & & & & & | \\ H_2 & -C- & OCOR''' & & & ROCOR''' & & H_2C-OH \\ & \text{Triglyceride} & & \text{Alcohol} & & \text{Biodiesel} & & \text{Glycerol} \end{array} \quad (1)$$

The terms methyl or ethyl are added to them when the alcohol used is methanol or ethanol. Several parameters influence the kinetics of this reaction. These include:

- The type and amount of catalyst used;
- The alcohol/oil or alcohol/fat ratio;
- Temperature;
- Reaction time;
- The stirring speed also called the stirring intensity.

Indeed, stoichiometry requires that the number of moles of the alcohol be three times the triglycerides of the oil used. To increase the speed of the reaction, an excess of alcohol is sometimes necessary [5].

The most important element that influences the rate of the reaction is the catalyst. When mixed with alcohol, alkyds are formed. On this, the stirring intensity influences the kinetics of the transesterification reaction [6].

However, the higher the stirring speed, the faster the reaction. The transesterification reaction must take place at a lower temperature but close to the boiling temperature of the alcohol used [6].

According to the literature review, Raphia oils consist of the following values:

The different solutions are obtained by digital simulation and modeling by implementing the different values obtained, the results of which Pamphile *et al.* 287 follow linear and exponential trend curves.

The different solutions are obtained by digital simulation and modeling by implementing the different values obtained, the results of which Pamphile *et al.* 287 follow linear and exponential trend curves. **Table 1** shows some acids and indices found in Raphia oils (source [4]).

3.2. Presentation of Equipment

The analysis being carried out using software, we present below the synthetic summary of the equipment constituting the production chain. On this, we highlight the appearance of their dimensions as well as the properties of the intrinsic materials. However, the equipment used is:

1) Mixer (Blender): The mixer module mixes multiple inlet jets and performs an instantaneous adiabatic calculation at the mixer output pressure [7].

2) Pump: The pump liquid module is used to increase the pressure of a liquid

Table 1. Raphia oil's composition.

Elements	Values
Palmitic acid (lauric acid))	37% to 38.5%
Oleic acid	6% to 7%
Linoleic acid	19.5% to 21%
Stearic acid	1% to 1.4%
Oil content	23% ± 3%
Density (20˚C)	0.930 ± 0.008
Refractive index	1.46668 ± 0.0004
Acid number	4.16 ± 1.08
Iodine value	82 ± 0.8

jet. Outlet pressure or pressure increase can be indicated. In either case, the work required is calculated [8].

3) UA simplex (one-inlet) heat exchanger is modeled according to the relation [9]:

$$Q = U \times A \times LMTD \tag{2}$$

With:

- U = overall heat transfer coefficient;
- A = heat exchanger section;
- $LMTD$ = logarithmic mean temperature difference.

4) RAMP, Unit Op is used to change various operating parameters with respect to time. In dynamic simulations, RAMP can be used to simulate operator functions such as opening a valve at time = t [10].

5) Reactor 1: The equilibrium reactor model gives the user the possibilities to simulate reactors with multiple reactions defined by conversion or equilibrium ratios [11]. Product rates, compositions, and thermal conditions can be calculated by solving the reactor equilibrium equation with given mass and energy balances [12]:

$$\ln\left(k_{eq}\right) = \ln\frac{\left(p_1\right)^{x_1} \times \left(p_2\right)^{x_2} \times \cdots \times \left(p_i\right)^{x_i}}{\left(R_1\right)^{y} \times \left(R_2\right)^{y_2} \times \cdots \times \left(R_j\right)^{y_j}} = A + \frac{B}{T} \tag{3}$$

where:

- P_i = partial pressure (if vapor) or mole fraction (if liquid) of product component i;
- R_j = partial pressure (if vapor) or mole fraction (if liquid) of reactant component j;
- x= power coefficient of the product component (always positive), usually equal to the stoichiometric coefficient;
- y = power coefficient of the reactant component), generally equal to the stoichiometric coefficient, always negative;
- A and B = coefficients for the equilibrium reaction equation;

- T = temperature, absolute degrees.

6) Distillation Column: SCDS is a rigorous multi-stage vapor-liquid equilibrium module that simulates any simple column calculation including distillation columns, absorbers and strippers. SCDS offers a variety of specifications, such as total mole rate, heat duty, reflux ratio, tip-up ratio, temperature, mole fraction, recovery fraction, component rate, and the flow ratio of two components in products [13].

7) Reactor 2: The kinetic reactor model allows to evaluate or design the intake flow and continuous stirred tank reactors up to 300 simultaneous reactions are permitted [14].

The total reaction rate for a single component in a simultaneous reaction is given by the following expression [14]:

$$r_i = \left(\sum_{j=1}^{nrx} N_{ij} \times A_j \times \mathrm{e}^{-E_i/(RT)} \times \prod_{k-1}^{N_i} \left(C_k\right)^{a_{ki}} \right) \times \left(1 + \sum_{k-1}^{n_i} \varphi_{kj} \times \mathrm{e}^{-E_i/(RT)} \times C_{kj}^{b_{ki}} \right)^{-\beta_i} \quad (4)$$

Within:

- r_i = formation rate for component i, mole/volume-time;
- i = subscript for component i;
- k = subscript for reactant k;
- j = subscript for reaction j;
- N_{ij} = stoichiometric coefficient for component i in reaction j;
- A_j : Frequency factor (Arrhenius parameter) in reaction j;
- E_{kj} : Activation energy in reaction j;
- R = universal gas constant;
- T = absolute temperature;
- C_k = concentration of reactant k, mole/volume or partial pressure of reactant k;
- a_{kj} : exponential factor for reactant k in reaction j;
- n: number of reactants;
- nrx: reaction number;
- kj: absorption frequency factor for component k (adsorption factor);
- j: power factor for the limit of absorption sites for reaction j (betas factors);
- b_{kj} : Exponential adsorption factor for reactant k in reaction j.

8) Wash column: The extraction module calculates the heat and mass equilibrium of contacting stage wise of two immiscible liquid mixtures [15]. This unit allows up to five feeds and six products. It allows up to 300 steps and accommodate step efficiencies. The extraction module uses the simultaneous Newton-Raphson convergence technique for its solution.

9) The separator serves as a black-box separator which splits an input stream into two product streams of different compositions and thermal conditions. Through either split indication fraction or throughput split component by component, almost any kind of separation can be performed [16].

3.3. Graphical and Analytical Expressions

The diagram being so complex, the result obtained graphically and numerically

comes from the fundamental equations of chemistry and fluid mechanics. Therefore, for this work, it is added to Equations (1)-(4), the equations as developed following the graphs.

3.3.1. Input Expressions

1) Properties

The diagram being so complex, the result obtained graphically and numerically comes from the fundamental equations of chemistry and fluid mechanics. Therefore, for this work, it is added to Equations (1)-(4), the equations as developed following the graphs. Table 2 shows the input expressions properties.

Table 2. Implementation input expressions and values.

Name	Raphia Oil	NaOH	Methanol
- - Overall - -			
Molar flow *kmol/h*	1.1861	0.2500	3.6577
Mass flow *kg/h*	1050.0650	10.0000	117.2000
Temp *C*	60.0000	25.0000	25.0000
Pres *bar*	1.0000	1.0000	1.0000
Vapor mole fraction	0.0000	0.0000	0.0000
Enth *MJ/h*	−2881.3	−201.89	−874.02
Tc C	1366.7945	2546.8500	239.4900
Pc bar	4.7057	253.3101	80.9700
Std. sp gr. *wtr = 1*	0.909	1.934	0.801
Std. sp gr. air = 1	30.568	1.381	1.106
Degree API	24.2283	−58.3469	45.2429
Average molwt	885.3232	39.9970	32.0420
Actual dens kg/m^3	885.0295	1913.3401	789.5790
Actual vol m^3/h	1.1865	0.0052	0.1484
Stdliq m^3/h	1.1557	0.0052	0.1464
Stdvap 0 C m^3/h	26.5844	5.6038	81.9824
--Liquid only--			
Molar flow *kmol/h*	1.1861	0.2500	3.6577
Mass flow *kg/h*	1050.0650	10.0000	117.2000
Average *molwt*	885.3232	39.9970	32.0420
Actual dens kg/m^3	885.0295	1913.3401	789.5790
Actual vol m^3/h	1.1865	0.0052	0.1484

Continued

Stdliq m^3/h	1.1557	0.0052	0.1464
Stdvap 0 C m^3/h	26.5844	5.6038	81.9824
Cp *kJ/kg-K*	1.8335	1.4720	2.5317
Z factor	0.0921	0.0033	0.0022
Visc $N\text{-}s/m^2$	0.001364	3.590	0.0005380
Thcond *W/m-K*	0.1713	0.3633	0.1999
Surf tens *N/m*	0.0059	0.5241	0.0222

2) Graphics

Taking a temperature range of 25˚C to 60˚C, the viscosity curves for oil, caustic soda and methanol respectively at the inlet, those graphs (a), (b) and (c) shown different variations of viscosity versus temperature at entry points (**Figure 1**).

3) Mathematical expression

In the case of this experiment, the viscosity is given by the formula [17]:

$$\mu = \frac{\upsilon}{\rho} \tag{5}$$

where:

μ is the dynamic viscosity;

υ is the kinematic viscosity;

ρ is the density of the liquid.

3.3.2. Expression of the Output

1) Properties (Methyl-ester)

Table 3 shows the output expressions of methyl-ester properties.

Indeed, the cetane number is used to assess the self-ignition capacity of a diesel fuel. It is calculated by the following Klopfenstein relation [18].

$$I_c = 58.1 + 2.15 \times \frac{n-3}{2} - 15.9 \times N \tag{6}$$

Indeed, the cetane number is used to assess the self-ignition capacity of a diesel fuel. It is calculated by the following Klopfenstein relation (15). Within:

- *n*:carbon number;
- *N*: the number of double bonds.

2) Graphics

Variation of viscosity as a function of temperature at point 23 of the system (**Figure 2**);

Variation of pressure as a function of temperature at point 23 of the system (**Figure 3**);

Figure 3. Variation of vapor pressure with temperature of Methyl ether;

Variation of surface tension as a function of temperature at point 23 of the system (**Figure 4**);

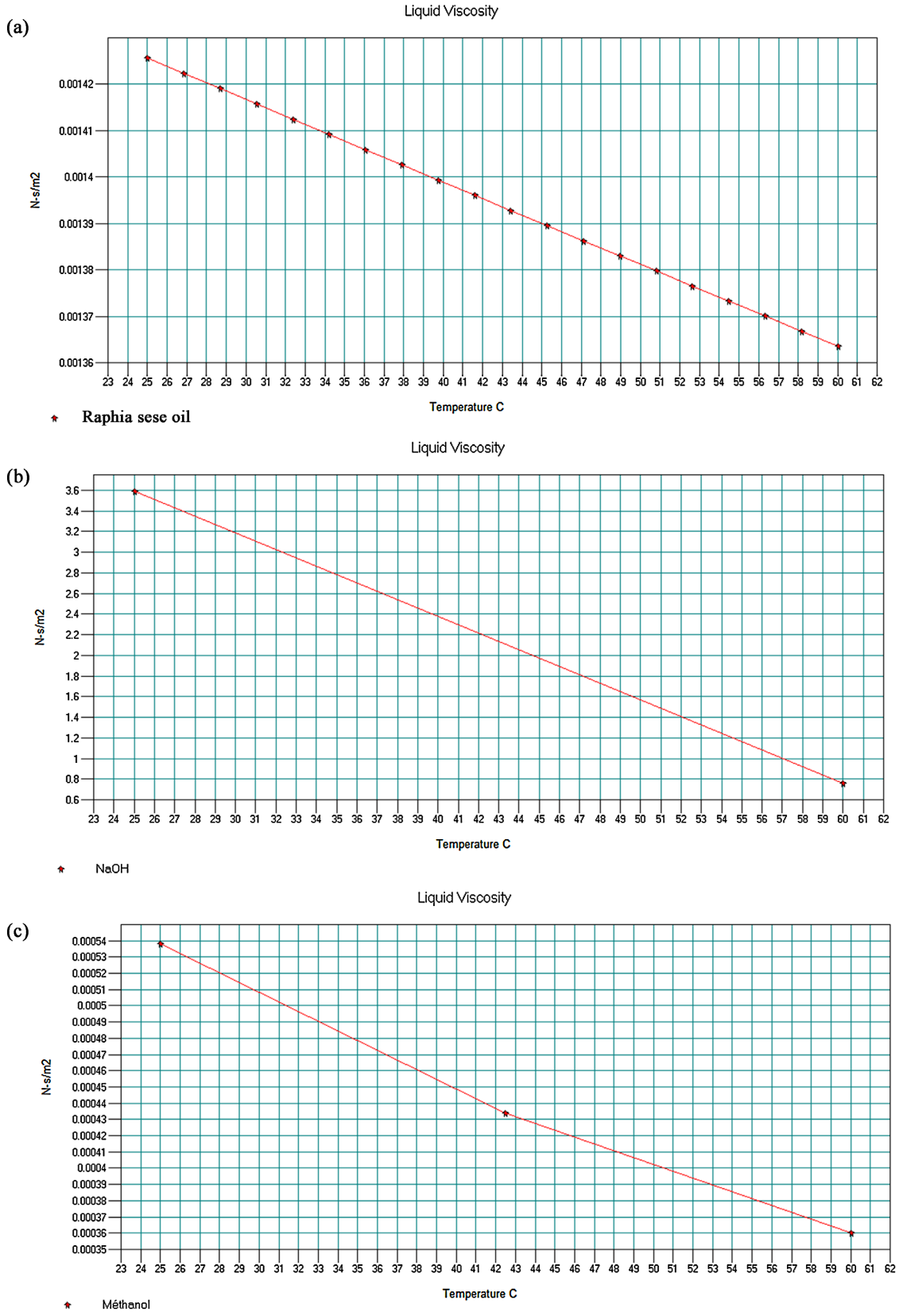

Figure 1. (a) Variation of viscosity liquid with temperature of raphia oil; (b) Variation of liquid viscosity with temperature of NaOH; (c) Variation of liquid viscosity with temperature of methanol.

Table 3. Expression of the output and values.

Molar flow kmol/h	2.3831
Mass flow kg/h	170.5228
Temp C	57.4944
Pres bar	1.0000
Vapor mole fraction	0.0000
Vapor mass fraction	0.0000
Enth MJ/h	−1650.3
Tc C	672.9142
Std. sp gr. wtr = 1	1.341
Std. sp gr. air = 1	2.471
Average mol wt	71.5555
Actual vol m^3/h	0.1296
Stdliq m^3/h	0.1271
Average mol wt	71.5555
Actualdens kg/m^3	885.2437
Stdliq m^3/h	0.1271
Stdvap 0 C m^3/h	53.4136
Cp kJ/kg-K	2.3589
Z factor	0.0032
Visc N-s/m^2	0.02026
Th cond W/m-K	0.3276
Surf tens N/m	0.0600
Degree API	−27.8086
Pour point C	−95.1835
Cetane index	49.5062

Variation of the amount of heat as a function of the temperature at point 23 of the system (**Figure 5**).

Shape of thermal conductivity as a function of temperature at point 23 of the system (**Figure 6**).

3) Math expressions

Classically, the equations that govern the movement of fluids in the production line are:

- Conservation of mass [19]:

$$\frac{\mathrm{d}\rho}{\mathrm{d}t} + \rho\nabla\cdot\boldsymbol{u} = 0 \tag{7}$$

- Conservation of momentum [20]:

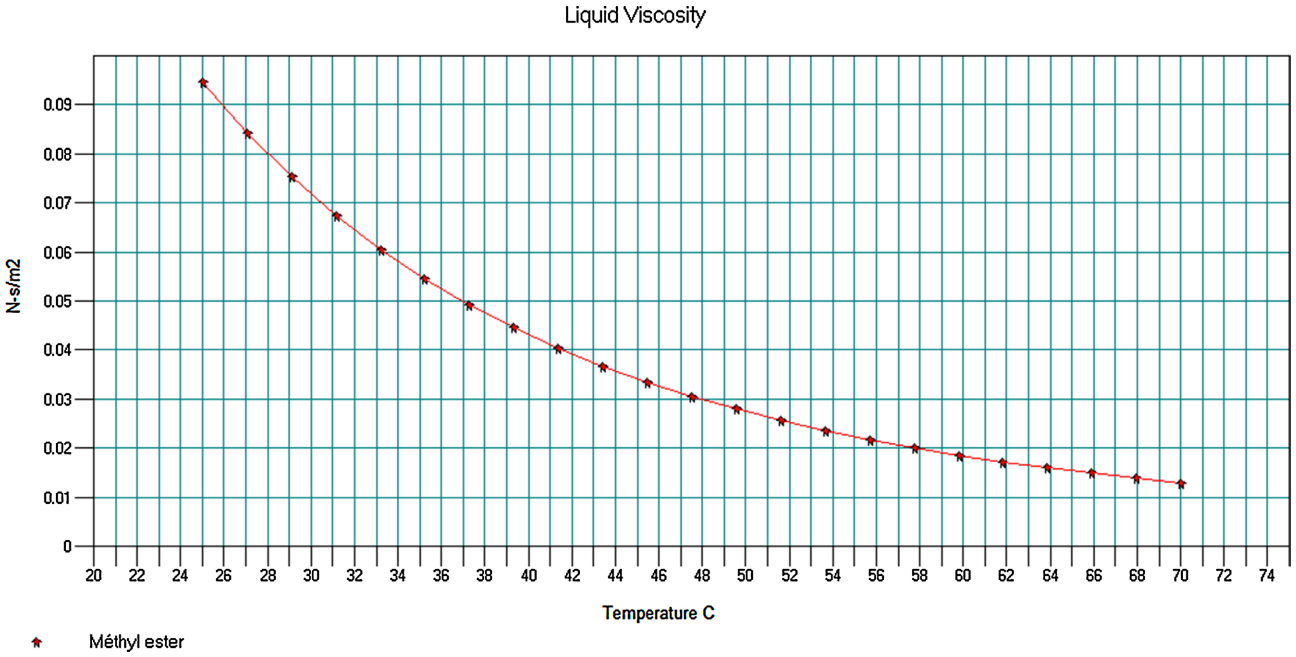

Figure 2. Variation of liquid viscosity with temperature of methyl ether.

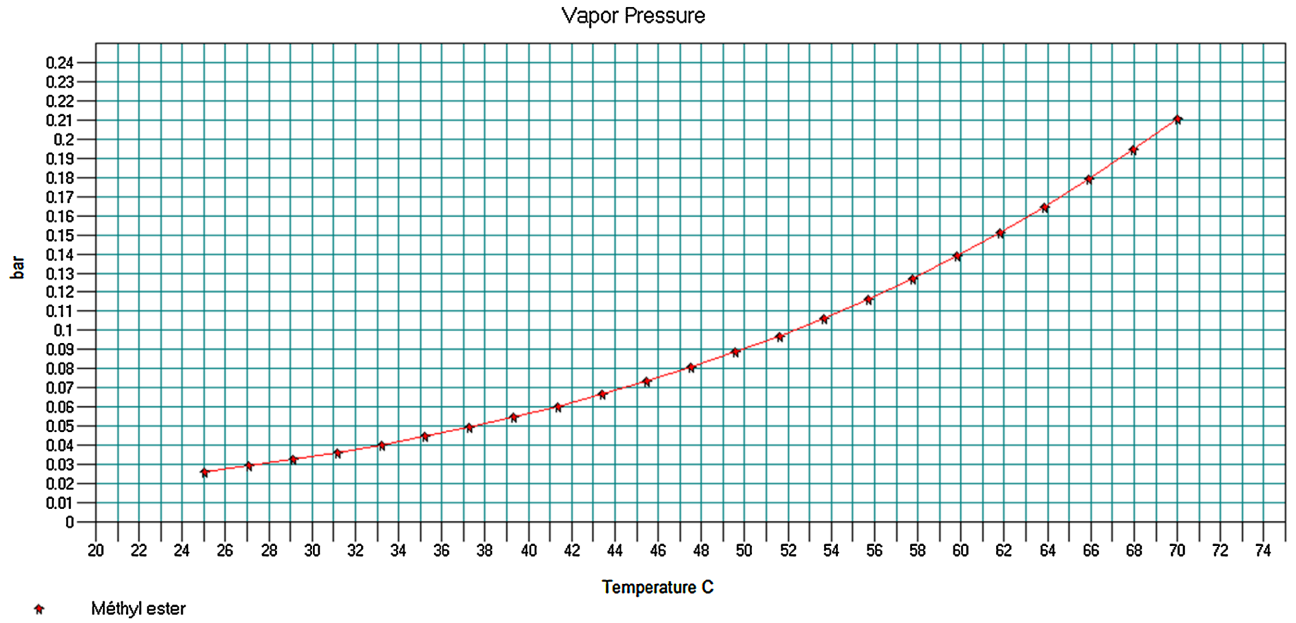

Figure 3. Variation of vapor pressure with temperature of methyl ether.

$$\rho \frac{\mathrm{d}u_i}{\mathrm{d}t} = \sum_{j=1}^{3} \frac{\partial \sigma_{ij}}{\partial x_j} + f_i \tag{8}$$

Whitin:

$$\sigma_{ij} = -p\delta_{ij} + \lambda \sum_{k=1}^{3} \varepsilon_{kk}(u)\delta_{ij} + 2\mu\varepsilon_{ij}(u) \tag{9}$$

where:

- $\boldsymbol{u}(x,t)$ is the velocity vector of components (u_1, u_2, u_3) in the frame;

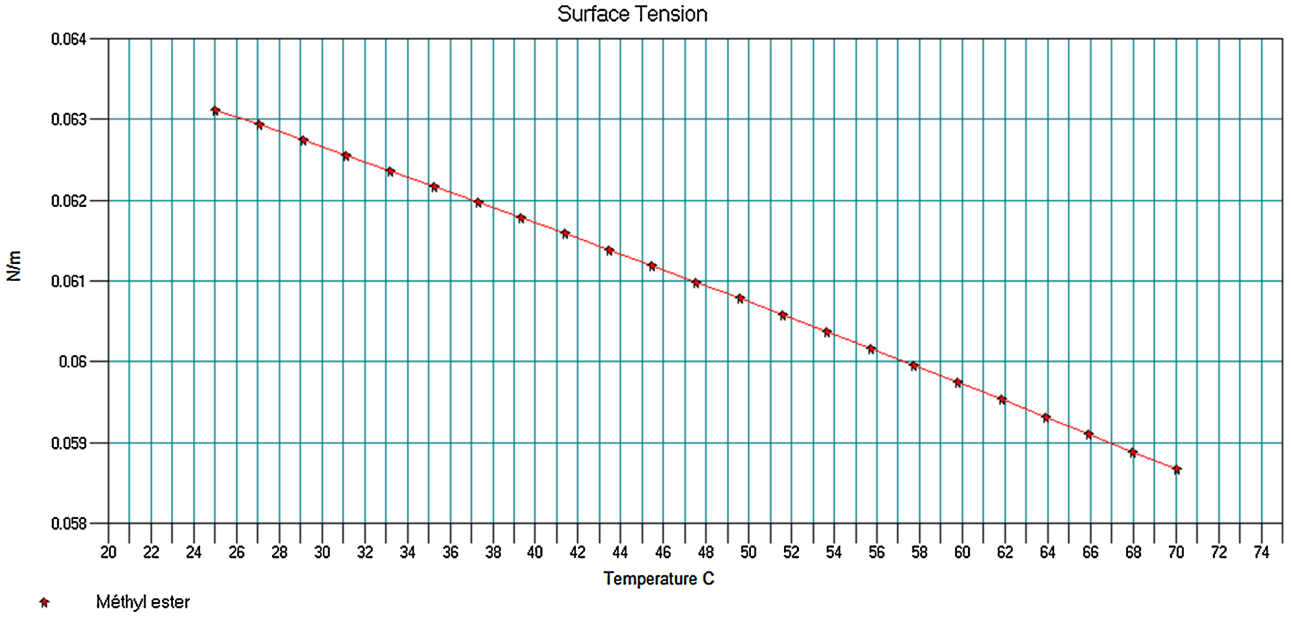

Figure 4. Variation of surface tension with temperature of methyl ether.

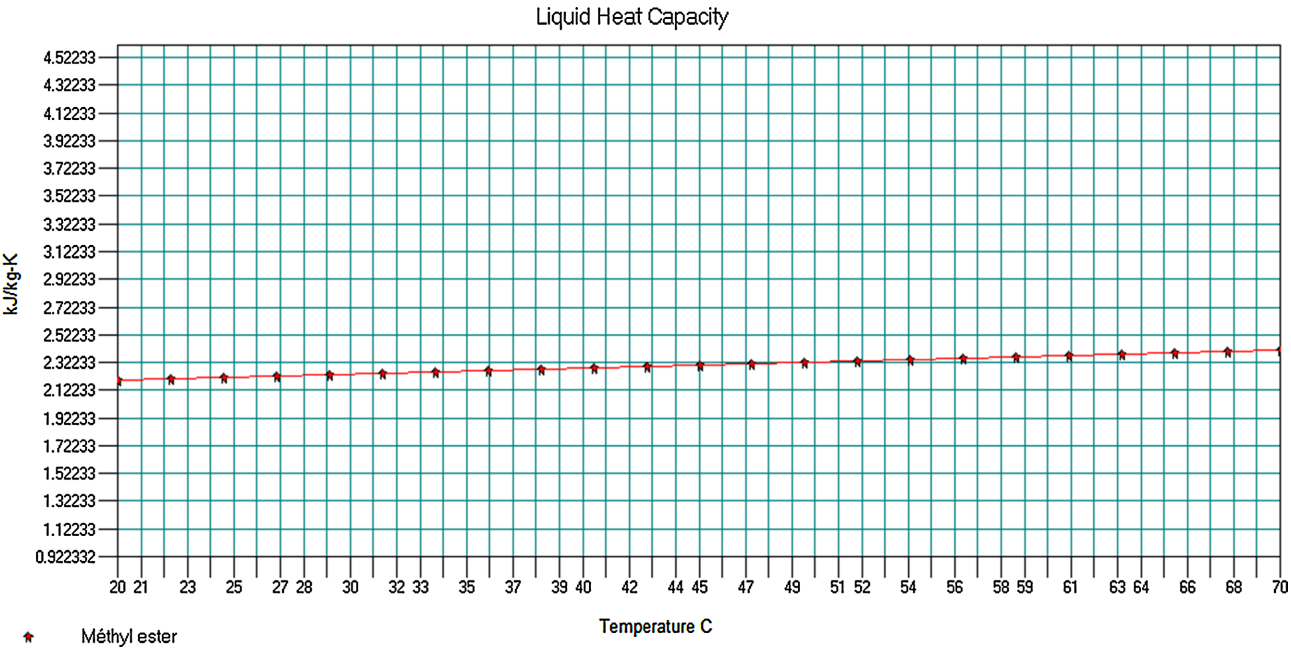

Figure 5. Variation of liquid heat capacity with temperature of methyl ether.

- $\boldsymbol{x} = (x_1, x_2, x_3)$ is the position vector (Euler coordinates) of the particle considered at time t;
- $\rho(\boldsymbol{x}, t)$ is the density;
- $\boldsymbol{f}(\boldsymbol{x}, t) = (f_1, f_2, f_3)$ is the volumetric density of the external forces acting on the fluid (generally the forces of gravity);
- $p(\boldsymbol{x}, t)$ is the fluid pressure;
- $\sigma_{ij}(\boldsymbol{x}, t)$ are the components of the symmetric stress tensor.

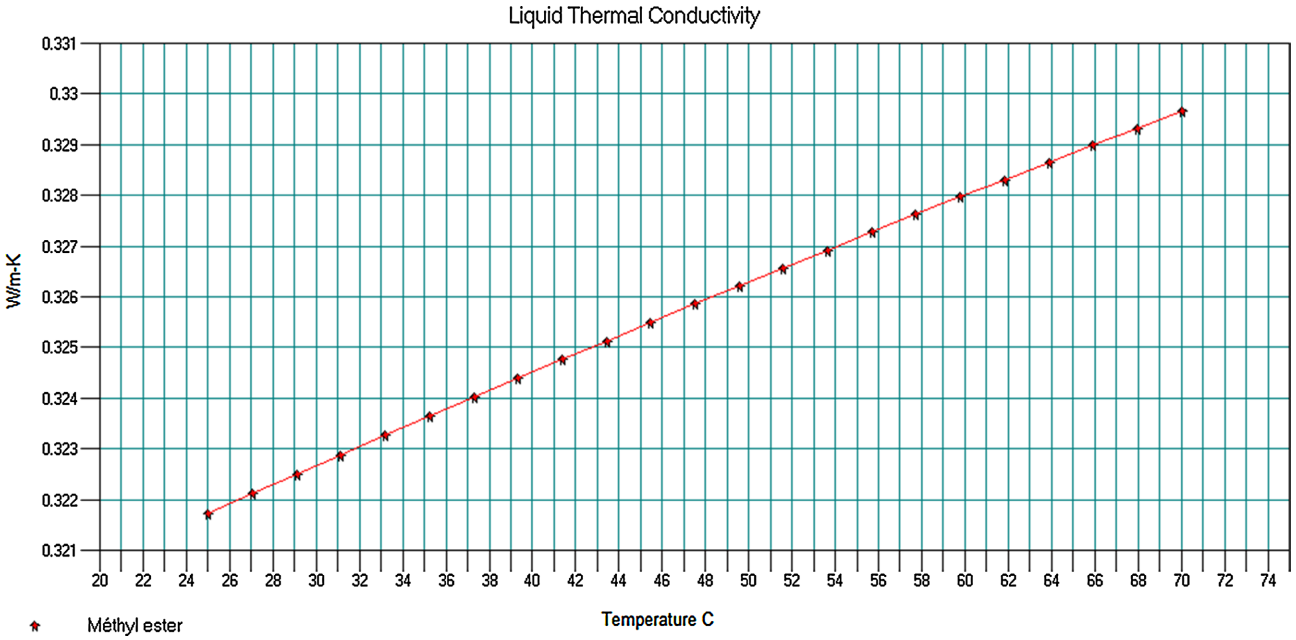

Figure 6. Variation of liquid thermal conductivity with temperature of methyl ether.

$$\varepsilon_{ij}(\mathbf{x},t)=\frac{1}{2}\left(\frac{\partial u_i}{\partial x_j}+\frac{\partial u_j}{\partial x_i}\right) \tag{10}$$

ε_{ij} is components of the strain rate tensor.

- λ and μ are coefficients of viscosity.

According to Navier-stokes:

The state law of an incompressible medium reads:

$$\nabla \cdot \boldsymbol{U}=0 \tag{11}$$

In this case:

$$\sigma_{ij}=-p\delta_{ij}+2\mu\varepsilon_{ij}(u) \tag{12}$$

The above equations are valid in the sections where there is only oil, catalyst or methanol. But, in a complex way, after each mixing, the pipes receive a fluid of variable *m*. Thereupon, the velocity profile is obtained by solving Equation (13) for variable.

$$\frac{\mathrm{d}v}{\mathrm{d}r}=\frac{-\frac{ar}{2}\left[\left(\frac{ar}{2}\right)^n+\left(\sigma_{ij}\right)^n\right]}{\left(\sigma_{ij}\right)\mu_0+\mu_\infty\left(\frac{ar}{2}\right)^n} \tag{13}$$

By simulating the variable very close to unity ($n=1$) the envelope result is:

The shape of the envelope as a function of the temperature at point 23 of the system (Figure 7).

However, the velocity profile will become:

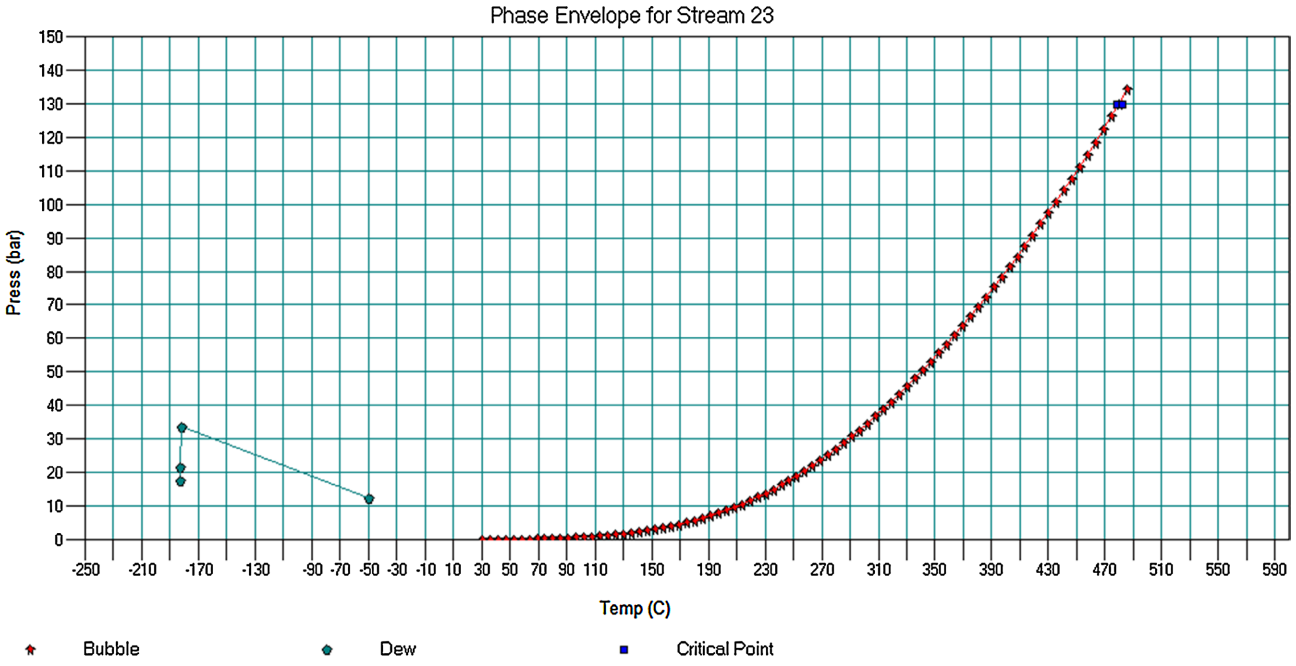

Figure 7. Variation of phase enveloppe for stream 23 with temperature of methyl ether.

$$\frac{\mathrm{d}v}{\mathrm{d}r} = \frac{-\frac{ar}{2}\left[\frac{ar}{2} + \sigma_{ij}\right]}{\left(\sigma_{ij}\right)\mu_0 + \mu_\infty\left(\frac{ar}{2}\right)} \tag{14}$$

4) Stress analysis

Expressions (13) and (14) are fluid velocity and pipe radius, respectively. Therefore, relation (14) gives the desired speed profile for biodiesel. Once the velocity profile has been found, the various stresses can be calculated taking into accounts the fluid-solid interaction, using the Phan-Thien and Tanner (MPTT) model, which is not the subject of our study. Thereupon, the constraint equation is obtained from the equilibrium equation in the form:

$$\lambda_{i0} = \frac{D\tau_{ij}}{Dt} + \sigma_i\left(tr\,\tau_{ij}\right)\tau_{ij} = 2\eta_m D \tag{15}$$

where:

τ_{ij} will be the shear stress, the macroscopic strain rate tensor, η_m the ratio of fluid viscosity and normal stress.

3.3.3. Sampled Test Values

Table 4 shows sampled test values of oil, methanol and caustic soda.

Table 4. Sampled test values of biodiesel's production.

Oil	Methanol	NaOH
250 g	70 g (stoichiometry)	2.5 g
	86 g (66% excess)	2.5 g

4. Conclusion

The purpose of the synthetic analysis was to present, using a chemcad calculator, the precise properties and evolutionary curves of a biodiesel resulting from the methanol-raphia oil interface. This representation model will serve as a standard of this kind of processes for any other oil and alcohol according to the need of the environment. A large number of tables have not been inserted due to compliance with publication standards. Nevertheless, the curves, the tables and the equations illustrated are effective in understanding because, to a certain extent of the chain.

Conflicts of Interest

The authors declare no conflicts of interest.

References

[1] Fapetu, O.P., Akinola, A.O., Lajide, L.L. and Osasona, A.B. (2018) Physicochemical Characteristics Study of Oil Extracted from Raffia Palm Seed. *Futa Journal of Engineering and Engineering Technology*, **12**, 102-114.

[2] (1992) Technique de l'ingénieur, traité génie énergétique, BE8550. Biocarburants.

[3] Srivastava, A. and Prasad, R. (2000) Triglycerides-Based Diesel Fuels. *Renewable and Sustainable Energy Reviews*, **4**, 111-133. https://doi.org/10.1016/S1364-0321(99)00013-1.

[4] Mbodo, N. (2017) Contribution aux procédés de transformation des huiles de raphia sese en biodiesel en vue de son utilisation dans un moteur hybride. Master's Thesis, Institute of Applied Techniques, Kinshasa.

[5] Hamad, B. (2009) Transestérification des huiles végétales par l'éthanol en conditions douces par catalyses hétérogènes acide et basique. Autre. Université Claude Bernard, Lyon I.

[6] Bancquart, S., Vanhove, C., Pouilloux, Y. and Barrault, J. (2001) The Synthesis of Monoglycerides through the Catalyzed Transesterification of Basic Oxides. *Oilseeds, Fats, Lipids*, **8**, 253-257.

[7] Hemrajani, R.R. and Tatterson, G.B. (2004) Mechanically Stirred Vessels. In: Paul, E.L., Atiemo-Obeng, V.A. and Kresta, S.M., Eds., *Handbook of Industrial Mixing: Science and Practice*, Wiley, 345. https://doi.org/10.1002/0471451452.ch6

[8] Simb, T.S. (2012) Fabrication d'une pompe manuelle. ISF Cameroun et CTA, coll. "PRO-AGRO". 28.

[9] Bontemps, A. and Fourmigué, J.-F. (2021) Analytical Calculation Methods. Heat Exchangers - Thermal Dimensioning. Réf: BE9517 v1.

[10] https://www.isa.au.dk/consys/Denmark/UserManuals/RampControl/RampControl.asp

[11] Pamphile, B.N., Jonathan, N.N., Vanshok, E. and Gédéon, E.N. (2022) Modeling and Simulation of Reactors in Plug Flow Reactor (PFR) and Packed Bed Reactor (PBR) Series for the Conversion of Methanol into Hydrocarbons. *African Journal of Environmental Science and Technology*, **16**, 286-294. https://doi.org/10.5897/AJEST2022.3091

[12] Soustelle, M. (2015) Équilibres chimiques. Vol. 4, Londres, ISTE Group, coll., Génie des procédés/Thermodynamique chimique approfondie, 196.

[13] https://www.google.com/amp/s/docplayer.fr/amp/10499735-Simulation-rigoureuse-

de-colonnes-scds.html

[14] Debacq, M. (2016) Génie de la Réaction Chimique: Réacteurs homogènes. Master. CGP215 "Génie de la réaction chimique & Évaluation économique des procédés", Cnam Paris, France.

[15] Arul Jayan, M. (2022) Department of Chemical Engineering, Sathyabama University, récupéré le 07 septembre 2022, Unit-4 of Single and Multiple Reactors for Multiple Reactions. https://chem.libretexts.org/Bookshelves/General_Chemistry/Map%3A_Chemistry_-_The_Central_Science_(Brown_et_al.)/14%3A_Chemical_Kinetics/14.06%3A_Reaction_Mechanisms

[16] https://patents.google.com/patent/EP0920894B1/en

[17] Bloomberg, M.R. and Strickland Jr., C.H. (2012) Guidelines for the Design and Construction of Stormwater Management Systems Developed by the New York City Department of Environmental Protection in consultation with the New York City Department of Buildings.

[18] https://www.legarrec.com/entreprise/pourquoi-et-comment-mesurer-la-viscosite-dunfluide/

[19] Klopfenstein, W.E. (1982) Estimation of Cetane Index for Esters of Fatty Acids. *Chemists' Society*, **59**, 531-533. https://doi.org/10.1007/BF02636316

[20] Okuň, L.B. (2009) Energy and Mass in Relativity Theory. World Scientific, 253.